

# Chapter 5

## Fusion barrier distributions for ${}^{6,7}\text{Li} + {}^{209}\text{Bi}$ systems

### 5.1 Introduction

The study of fusion reactions with unstable nuclei and/or weakly bound stable nuclei ( ${}^{6,7}\text{Li}$  and  ${}^9\text{Be}$ ) is of great importance for the synthesis of super heavy elements and for the study of astrophysical processes. The structure of interacting (projectile/target) nuclei as well as impact from the coupling of breakup and nucleon transfer channels affects the fusion barrier. Thus, the enhancement or suppression in the fusion cross sections can occur at near the Coulomb barrier energy. Due to the low breakup threshold energy of weakly bound nuclei, the fusion barrier may increase and hence suppress the fusion cross sections. For weakly bound nuclei, about  $\sim 30\%$  suppression in fusion cross sections is observed at above the Coulomb barrier energy.

There are two different methods to obtain the fusion barrier distributions such as: (1) Using the fusion cross sections (2) Using quasi-elastic excitation functions. To extract the fusion barrier distributions from the fusion excitation function, high accuracy data are required. This is because one has to take double derivative of the

measured fusion cross sections. While in the case of quasi-elastic excitation functions, one has to deal with the single derivative of quasi-elastic excitation functions. This complementarity of fusion barrier distributions obtained from quasi-elastic scattering and fusion are due to the fact that the ratio of  $d\sigma^{qel}/d\sigma^R(E)$  at  $180^\circ$ , is the reflection coefficient  $R_o$  for  $l=0$  and the barrier penetration probability,  $T_o$ , related to fusion is unitary. Thus,

$$R^{qel}(E) + T^{fus}(E) = 1. \quad (5.1)$$

From this equation, it is understood that if new reaction channels other than quasi-elastic scattering and fusion are present, the  $T_o = 1 - R_o$ , no more represents fusion barrier penetration probability rather it gives the capture probability. This can be justified for the barrier distributions that are derived from quasi-elastic scattering at backward angles, in the reactions involving loosely bound nuclei, where breakup channel is dominant. Earlier, it was suggested that in the case of very heavy target-projectile systems, the barrier distributions from quasi-elastic scattering, leads to information about the total reaction threshold distribution, instead of the usually accepted information about the fusion barrier. This is due to the appearance of deep inelastic scattering besides quasi-elastic scattering and fusion in these systems [84]. Thus, while dealing with weakly bound nuclei, it is required to include the direct breakup channels and other breakup channels triggered by transfer reactions to the quasi-elastic excitation functions for the correct representation of fusion barrier distribution.

### 5.1.1 Present work

In the present work, fusion barrier distributions have been obtained from the measurement of the quasi-elastic scattering excitation functions at backward angle in the reactions of  ${}^6,{}^7\text{Li}$  with  ${}^{209}\text{Bi}$ . The fusion barrier distributions obtained from the quasi-elastic scattering excitation functions have been compared with the fusion barrier distributions which are extracted from the experimentally measured fusion cross sections. The comparisons were done by considering elastic + inelastic

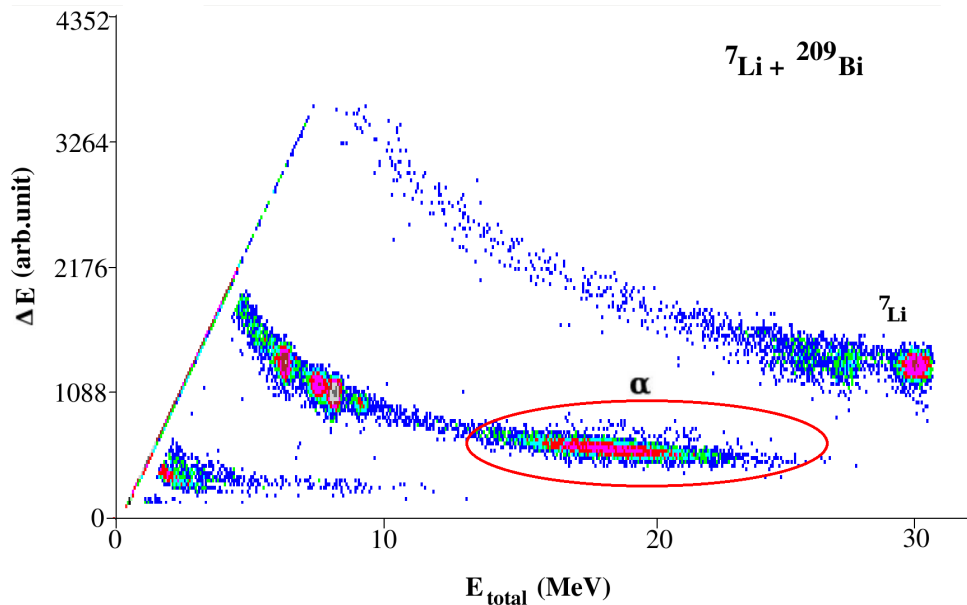


FIGURE 5.1: A typical bi parametric spectrum of  $\Delta E$  versus  $E_{total}$  in the reaction of  $^7\text{Li}$  with  $^{209}\text{Bi}$  for  $E_{lab} = 34$  MeV and  $\theta_{lab} = 140^\circ$ .

and elastic + inelastic + (breakup(BU) and/or transfer) and also from fusion excitation function measurements. The measurement were carried out at  $\theta_{lab} = 140^\circ$  and  $160^\circ$ . The fusion barrier distribution from fusion excitation function for  $^{6,7}\text{Li} + ^{209}\text{Bi}$  systems are available in the literature [85]. The coupled channels calculations are also carried out by considering different formalisms using FRESKO code [42]. The experimentally observed results of quasi-elastic scattering excitation function and corresponding barrier distributions for  $^{6,7}\text{Li} + ^{209}\text{Bi}$  systems were interpreted in terms of the coupled channels calculations.

## 5.2 Experimental Details

The present experiment have been performed at the 14UD BARC-TIFR Pelletron facility (see the sec.4.1.2), using  $^{6,7}\text{Li}^{(3+)}$  beams. For the experiment, a self supported  $^{209}\text{Bi}$  target of thickness  $\sim 1.2$  mg/cm<sup>2</sup> was used. The measurements have been done at two different backward angles that are,  $140^\circ$  and  $160^\circ$ . Two solid state surface barrier (SSB) detector telescopes that consist of thin  $\Delta E$  and thick  $E$  detector, were fixed on the rotating arm inside the scattering chamber of 1m diameter. The picture of scattering chamber is shown in the Fig.5.2. The thickness

of the detector telescopes were as follows: (1) Telescope ( $T_1$ ) with the thickness  $\Delta E = 15 \mu\text{m}$  and  $E=1.5 \text{ mm}$ . (2) Telescope ( $T_2$ ) with the thickness  $\Delta E = 25 \mu\text{m}$  and  $E=2 \text{ mm}$ . Two monitor detectors were placed at  $\pm 18^\circ$  for normalization and beam monitoring. The measurements were done in the bombarding energy range from 22.0 to 39.0 MeV in steps of 1.0 MeV. The bombarding energies have been corrected for the energy loss in half the target thickness, ranging from 0.12 to 0.18 MeV for  ${}^6\text{Li}$  and 0.14 to 0.2 MeV for  ${}^7\text{Li}$  projectile. Also, the results of quasi-elastic at  $140^\circ$  have been converted to that of  $180^\circ$  by introducing an effective energy [24], into the quasi-elastic cross sections that is,

$$E_{eff} = \frac{2E_{c.m.}}{[1 + \text{cosec}(\theta_{c.m.}/2)]}. \quad (5.2)$$

Thus, the centrifugal corrections were introduced by making,

$$\sigma_{qe}(E_{eff}) \approx \sigma_{qe}(E_{c.m.}, 140^\circ) \quad (5.3)$$

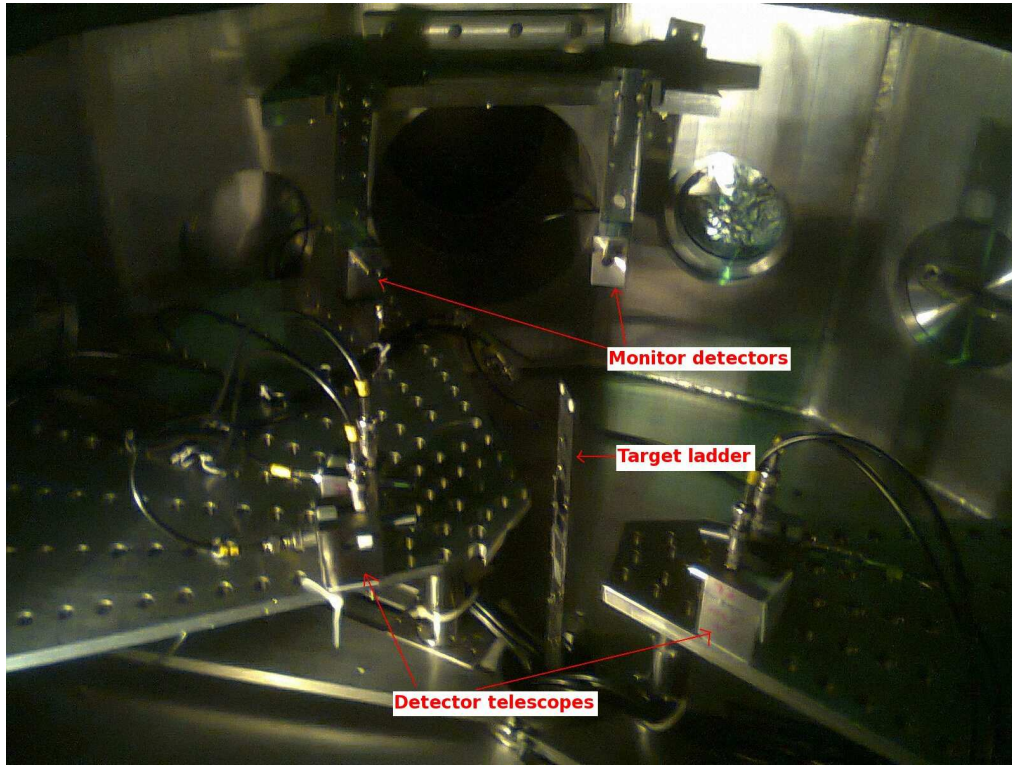


FIGURE 5.2: A picture of scattering chamber and detector telescopes.

A block diagram of electronic setup for the present measurement was similar to the one, as shown in the Fig.3.5 (See Chapter 3). However, in the present measurement only two detector telescope were used. A typical two dimensional  $\Delta E$  versus  $E_{total}$  spectrum that have been obtained at  $\theta_{lab} = 140^\circ$  and  $E_{lab} = 34$  MeV for  $^7\text{Li} + ^{209}\text{Bi}$  system, is shown in the Fig. 5.1. ‘LAMPS’ software has been used to perform all the experimental data analysis.

## 5.3 Data Analysis

### 5.3.1 Quasi elastic scattering excitation functions

In order to obtain the quasi elastic scattering excitation functions, the elastic, inelastic and breakup- $\alpha$  channels have been considered as quasi-elastic channel and divided it with  $\sigma_{Ruth}$  for both the  $^{6,7}\text{Li} + ^{209}\text{Bi}$  systems.

In the Fig. 5.1, a distinct blob of  $\alpha$ -particle yield can be clearly seen, peaking at  $4/7$  of lab energy for the reaction of  $^7\text{Li}$  with  $^{209}\text{Bi}$ . That has widths around  $\sim 8$ - $10$  MeV and  $\sim 13$ - $17$  MeV for  $^{6,7}\text{Li} + ^{209}\text{Bi}$  systems, at different projectile energies. These widths are calculated using the kinematics relation for both the  $^{6,7}\text{Li} + ^{209}\text{Bi}$  systems as given in Ref. [86]. Thus, the contributed  $\alpha$ -yields were considered for the quasi-elastic channel. For reactions of  $^{6,7}\text{Li}$  with  $^{209}\text{Bi}$  the probability of alpha particles coming from the direct reactions can have different origins mainly direct breakup ( $\alpha + d$  or  $\alpha + t$ ) of projectiles ( $^{6,7}\text{Li}$ ) or breakup of projectile followed by  $1p$ -pick up,  $1n, 2n$ -stripping in case of  $^7\text{Li}$  projectile. Also, for  $^6\text{Li} + ^{209}\text{Bi}$  system the BU of projectile may occur via direct breakup,  $1p, 1n$ -pick up,  $1n$ -stripping [87]. The statistical model calculations show that the  $\alpha$ -particle coming from the evaporation are lower in energies. Using the kinematics, impurities coming from  $^{16}\text{O}$  and  $^{12}\text{C}$  in the observed  $\alpha$ -particle energy peaks of our considerations are also checked. It has been observed that the breakup  $\alpha$ -peaks from the contamination of  $^{16}\text{O}$  and  $^{12}\text{C}$  fall below the 9.0 MeV, while for the present reactions of  $^{6,7}\text{Li}$  with  $^{209}\text{Bi}$  target peak at 20.38 and 17.18 MeV respectively. In this way, the contributed

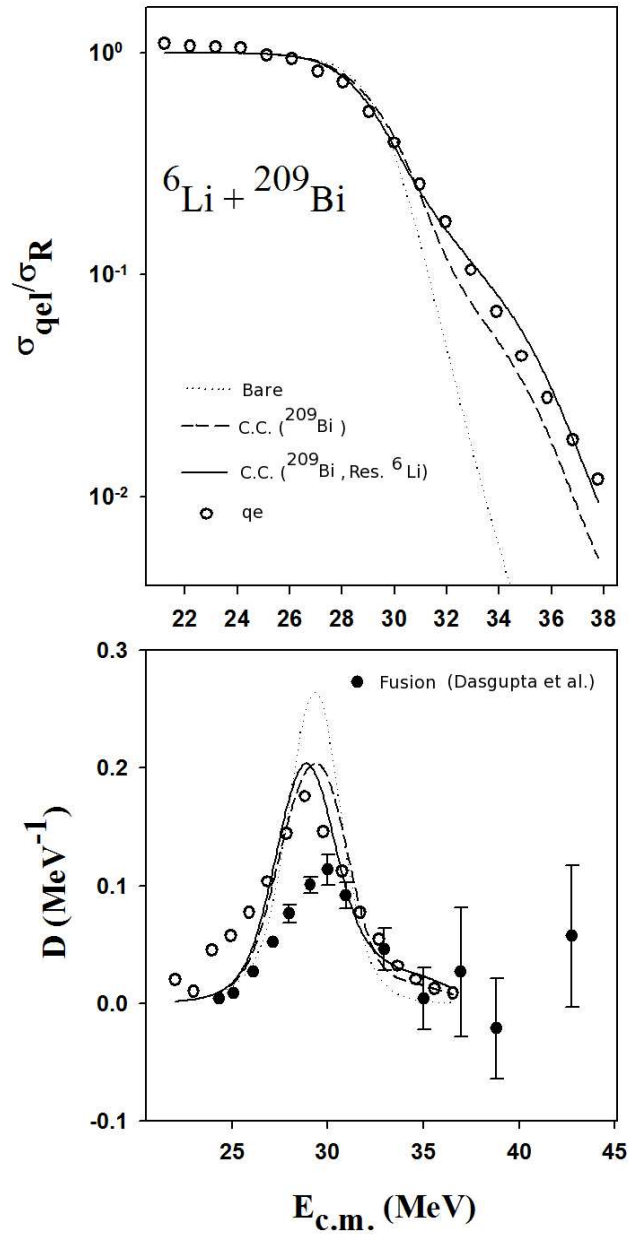


FIGURE 5.3: (a) Quasi-elastic scattering excitation function and (b) corresponding fusion barrier distributions along with the CC calculations, for  ${}^6\text{Li} + {}^{209}\text{Bi}$  system at  $160^\circ$ . The dotted and dashed lines represent the calculations without coupling and with the inclusion of target inelastic excitations respectively. The CC calculations with inclusion of both the target inelastic excitations and projectile resonant states are shown by continuous lines.

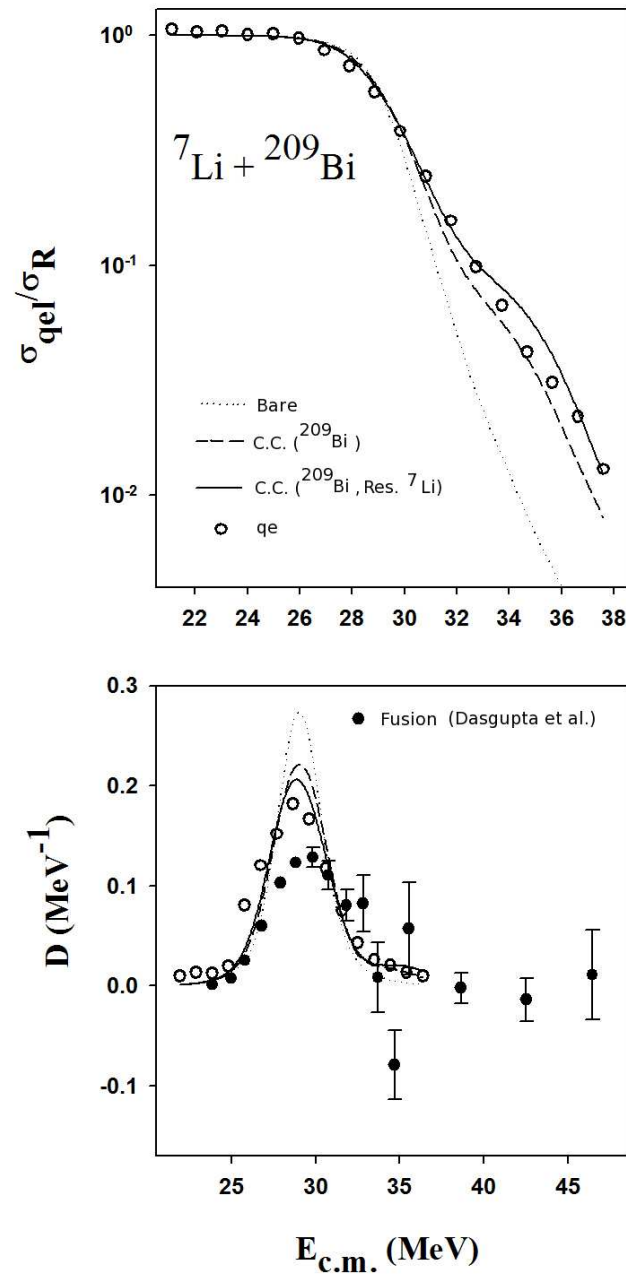


FIGURE 5.4: (a) Quasi-elastic scattering excitation function and (b) corresponding fusion barrier distributions along with the CC calculations, for  ${}^6\text{Li} + {}^{209}\text{Bi}$  system at  $160^\circ$ . The dotted and dashed lines represent the calculations without coupling and with the inclusion of target inelastic excitations respectively. The CC calculations with inclusion of both the target inelastic excitations and projectile resonant states are shown by continuous lines.

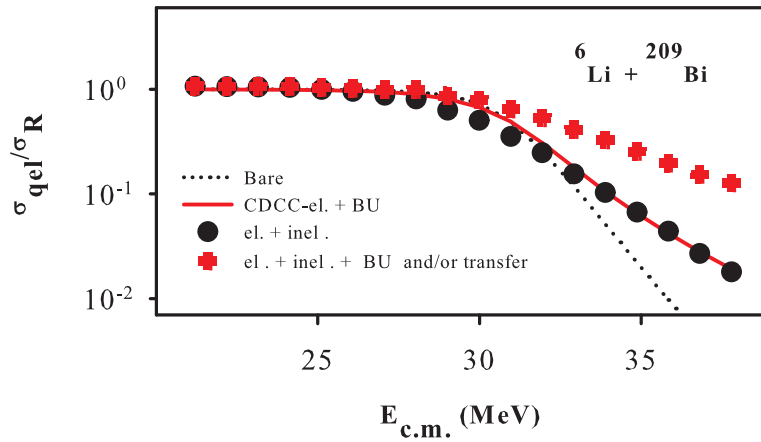


FIGURE 5.5: Quasi-elastic scattering excitation function for  ${}^6\text{Li} + {}^{209}\text{Bi}$  system at  $140^\circ$ . The filled circles (black) show the data points with elastic + inelastic and crosses (red) show the the data points with elastic + inelastic + BU and/or transfer. The dotted line indicates the results of Coupled Channels calculations using bare potential. The continuous line shows the results from CDCC calculation which includes elastic + direct breakup(BU).

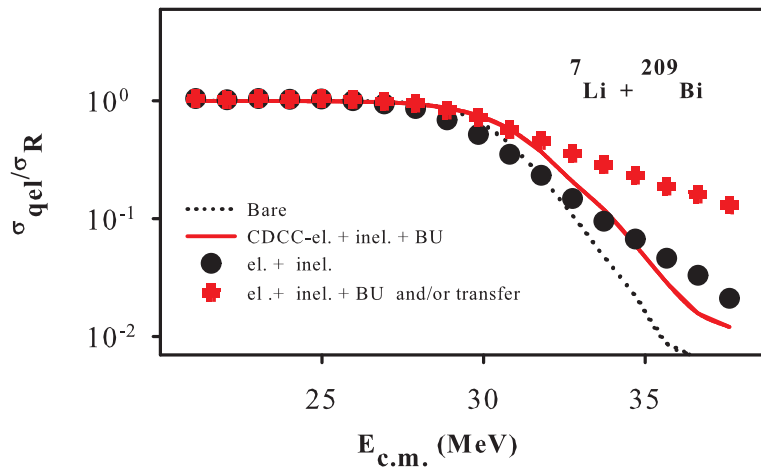


FIGURE 5.6: Quasi-elastic scattering excitation function for  ${}^7\text{Li} + {}^{209}\text{Bi}$  system at  $140^\circ$ . The filled circles (black) show the data points with elastic + inelastic and crosses (red) show the the data points with elastic + inelastic + BU and/or transfer. The dotted line indicates the results of Coupled Channels calculations using bare potential. The continuous line shows the results from CDCC calculation which includes elastic +  ${}^7\text{Li}$ -inelastic + direct breakup(BU).

$\alpha$ -particles are purely produced from the reactions of  $^{6,7}\text{Li}$  with  $^{209}\text{Bi}$ . Thus, in the present work, in order to understand the projectile breakup effects (via breakup and/or transfer) on fusion barrier distributions, these  $\alpha$ -particle yields have been taken as part of quasi-elastic scattering for both the  $^{6,7}\text{Li}$  with  $^{209}\text{Bi}$  reactions. The measured quasi-elastic excitation functions for both the  $^{6,7}\text{Li} + ^{209}\text{Bi}$  reactions have been shown in Figs. 5.5 and 5.6.

### 5.3.2 Derivation of fusion barrier distributions

From quasi-elastic excitation functions fusion barrier distributions have been extracted by taking 2.0 MeV energy steps, following the procedure described in the Ref. [24](See Sec.2.7). To extract the fusion barrier distributions from the obtained quasi-elastic excitation functions, a single derivative was taken. This quasi-elastic excitation functions includes elastic, inelastic and  $\alpha$  (breakup and/or transfer). The resulted fusion barrier distributions were compared with the one that have been obtained from the fusion excitation function for  $^{6,7}\text{Li} + ^{209}\text{Bi}$  systems which is available in the Ref.[85]. The obtained fusion barrier distributions for both the  $^{6,7}\text{Li} + ^{209}\text{Bi}$  reactions are shown in the Figs. 5.7 and 5.8. It is observed that the extracted fusion barrier distributions from the quasi-elastic (elastic + inelastic) scattering excitation functions are shifted to lower energy sides approximately by 1.21 MeV and 1.1 MeV as compared to the fusion barrier distributions which are extracted from the experimentally measured fusion cross sections, for  $^{6,7}\text{Li}$  respectively.

### 5.3.3 Transmission probability ( $T_{\circ}$ )

The transmission or capture probability ( $T_{\circ}$ ) has been extracted for the present quasi-elastic excitation function using the relation  $R^{qel}(E) + T^{fus}(E) = 1$  and also from the fusion excitation function by using the relation given below[85],

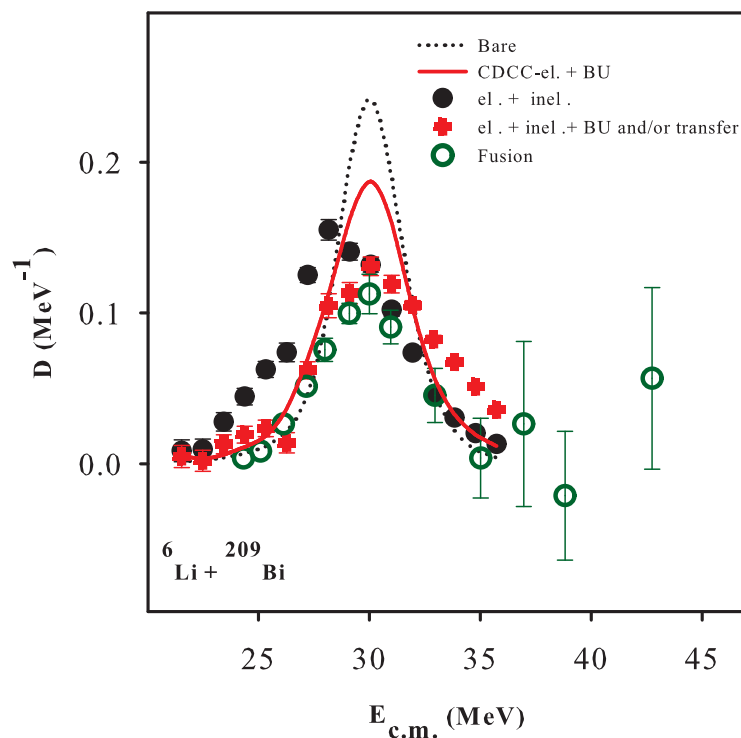


FIGURE 5.7: Fusion barrier distributions for  ${}^6\text{Li} + {}^{209}\text{Bi}$  system at  $140^\circ$ . The filled circles (black) show the data points with elastic + inelastic and crosses (red) show the the data points with elastic + inelastic + BU and/or transfer. The data points shown by unfilled circles are taken from the Ref.[85]. The dotted line indicates the results of Coupled Channels calculations using bare potential. The continuous line shows the results from CDCC calculation which includes elastic + direct breakup(BU).

$$T^{fus}(E) = \frac{1}{\pi R_b^2} \frac{d(\sigma.E)}{dE}. \quad (5.4)$$

Figs. 5.9 and 5.10 represent the transmission or capture probabilities( $T_o$ ) for both the reactions of  ${}^{6,7}\text{Li}$  with  ${}^{209}\text{Bi}$ . The transmission or capture probabilities which are derived from the fusion excitation functions indicate good agreement with the one from the present quasi-elastic scattering data excepting at well above the Coulomb barrier energies for  ${}^{6,7}\text{Li} + {}^{209}\text{Bi}$  reactions. The ( $T_o$ ) curves obtained from quasi-elastic scattering corresponding to elastic+inelastic channels and elastic+inelastic+ BU and/or transfer channels have overall shift in their energy positions. The observed shift is more for  ${}^6\text{Li} + {}^{209}\text{Bi}$  reaction compared to  ${}^7\text{Li} + {}^{209}\text{Bi}$  reaction which is co related with the projectile breakup threshold energy. This

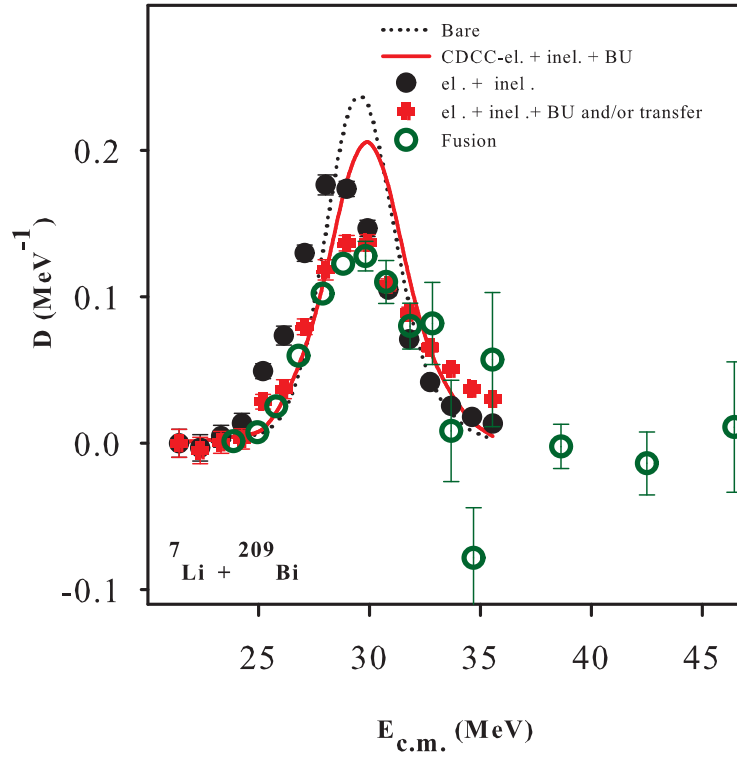


FIGURE 5.8: Fusion barrier distributions for  ${}^7\text{Li} + {}^{209}\text{Bi}$  system at  $140^\circ$ . The filled circles (black) show the data points with elastic + inelastic and crosses (red) show the the data points with elastic + inelastic + BU and/or transfer. The data points shown by unfilled circles are taken from the Ref.[85]. The dotted line indicates the results of Coupled Channels calculations using bare potential. The continuous line shows the results from CDCC calculation which includes elastic +  ${}^7\text{Li}$ -inelastic + direct breakup(BU).

suggests that due to the lower breakup threshold the energy shift is more in case of  ${}^6\text{Li}$ .

## 5.4 Theoretical Analysis

In order to understand the breakup and/or transfer channels coupling effect on fusion barrier distributions and hence on fusion cross sections at around the Coulomb barrier energy, coupled channels calculations have been carried out for  ${}^6,{}^7\text{Li} + {}^{209}\text{Bi}$  reactions using FRESKO code.

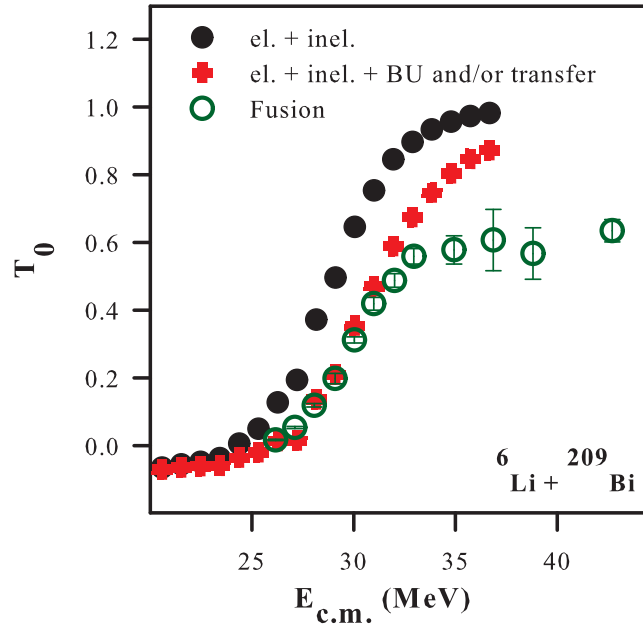


FIGURE 5.9: Transmission or capture probability ( $T_0$ ) as a function of  $E_{c.m.}$  in the reaction of  ${}^6\text{Li}$  with  ${}^{209}\text{Bi}$ . The filled circles (black) show the data points with elastic + inelastic and crosses (red) show the the data points with elastic + inelastic + BU and/or transfer. The data points shown by unfilled circles are taken from the Ref. [85]

### 5.4.1 Simple Coupled Channels calculation

In these type of calculations only the coupling of inelastic excitations are considered for both the projectiles( ${}^6,7\text{Li}$ ) and target( ${}^{209}\text{Bi}$ ). The required optical potentials in the present calculations are of Woods-Saxon (WS) form with parameters ( $V_o = 31.95$  MeV,  $r_o = 1.2$  fm,  $a_o = 0.76$  fm) and ( $V_o = 36.95$  MeV,  $r_o = 1.2$  fm,  $a_o = 0.70$  fm) for both the projectiles ( ${}^6,7\text{Li}$ ) scattering respectively. The imaginary part was an internal Woods-Saxon (WS) potential with  $W_o = 10.0$  MeV,  $r_o = 1.04$  fm and  $a_o = 0.4$  fm, to exclude the double counting of the effect of inelastic excitations on the elastic channel. Table 5.1 gives the inelastic excitations that are included in the Coupled Channels (CC) calculations as done in the Ref.[88]. In the calculations the energy steps are kept same as for the experimental measurements to avoid the ambiguities in comparison. In the Figs. 5.3 and 5.4, dotted and dashed lines show the results from bare potential and CC calculations with inclusion of target inelastic excitations only. The continuous lines show the CC calculations with

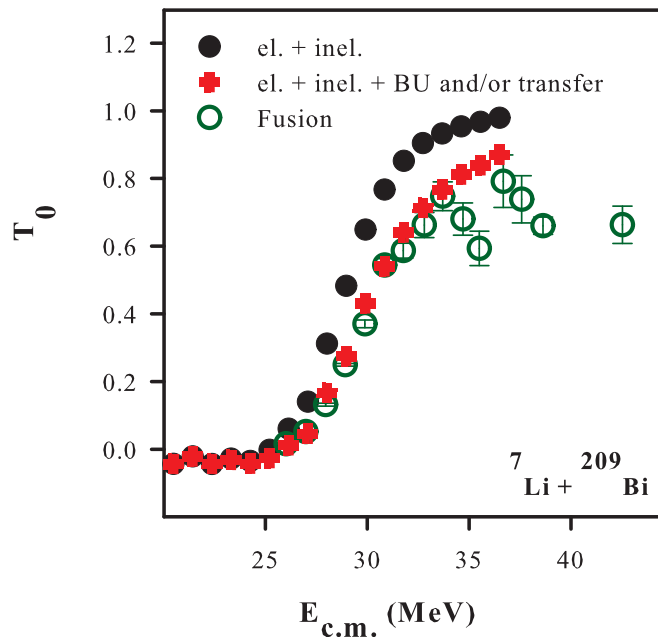


FIGURE 5.10: Transmission or capture probability ( $T_0$ ) as a function of  $E_{c.m.}$  in the reaction of  ${}^7\text{Li}$  with  ${}^{209}\text{Bi}$ . The filled circles (black) show the data points with elastic + inelastic and crosses (red) show the the data points with elastic + inelastic + BU and/or transfer. The data points shown by unfilled circles are taken from the Ref. [85]

TABLE 5.1: Inelastic excitations included in the Coupled Channels (CC) calculations

Nucleus	State	Energy(MeV)	$\beta$	References
${}^6\text{Li}$	$3^+$	2.18	0.87	[39]
${}^7\text{Li}$	$(1/2)^-$	0.478	0.89	[68]
${}^7\text{Li}$	$(7/2)^-$	4.63	0.89	[68]
${}^{209}\text{Bi}$	$3^-$	2.62	0.122	[89]
${}^{209}\text{Bi}$	$5^-$	3.09	0.0802	[89]
${}^{209}\text{Bi}$	$2^+$	4.18	0.05	[89]

inclusion of both the target inelastic excitations and projectile resonant states. From this figures, it is observed that the quasi-elastic excitation functions and the corresponding fusion barrier distributions are described reasonably well by the inclusion of  ${}^6,{}^7\text{Li}$  resonant states. This indicates that the breakup channel dominates as projectile resonant states are required to explain the quasi-elastic scattering excitation function.

TABLE 5.2: Total reaction ( $\sigma_{react.}^{total}$ ), integrated breakup ( $\sigma_{BU}^{inte.}$ ) and breakup cross sections at  $140^\circ$  ( $\sigma_{BU}^{140^\circ}$ ) from the CDCC calculation and  $\alpha$  cross sections at  $140^\circ$  ( $\sigma_\alpha^{140^\circ}$ ) from the experiment for  ${}^6\text{Li} + {}^{209}\text{Bi}$  system.

$E_{c.m.}$ (MeV)	$\sigma_{react.}^{total}$ (mb) (CDCC)	$\sigma_{BU}^{inte.}$ (mb) (CDCC)	$\sigma_{BU}^{140^\circ}$ (mb/sr) (CDCC)	$\sigma_\alpha^{140^\circ}$ (mb/sr) ( <i>Expt.</i> )
21.21	13	7	1.3	1±0.0
22.19	18	12	1.3	2±0.0
23.16	24	16	1.5	2±0.0
24.14	30	20	1.6	4±0.0
25.12	38	24	1.9	7±0.0
26.09	48	30	2.4	10±0.0
27.07	62	36	2.9	16±0.0
28.04	81	42	2.4	23±0.0
29.02	114	47	2.4	28±0.01
29.99	165	54	3.0	32±0.01
30.97	238	63	3.3	31±0.02
31.94	328	71	2.9	28±0.02
32.92	425	79	2.4	24±0.04
33.89	520	86	2.2	20±0.06
34.87	613	93	1.9	16±0.11
35.84	701	100	1.6	12±0.22
36.81	787	107	1.3	9±0.43
37.79	868	113	0.9	8±0.61

## 5.4.2 Continuum Discretized Coupled-Channels (CDCC) Calculations

The Continuum Discretized Coupled-Channels (CDCC) Calculations have been carried out to investigate the breakup coupling effects on the fusion barrier distributions for  ${}^6,{}^7\text{Li} + {}^{209}\text{Bi}$  systems. In this calculations, the projectiles  ${}^6,{}^7\text{Li}$  have been considered as  $\alpha + d/t$  clusters respectively. The continuum parts have been discretized in small momentum bins for non resonant parts and further fine binning have been done in resonant parts for both the  ${}^6,{}^7\text{Li}$  excitations. The maximum excitation energy has been taken up to  $\sim 9$  MeV and reduced to lower excitation for below and at the Coulomb barrier energies in the reactions of  ${}^6,{}^7\text{Li} + {}^{209}\text{Bi}$ . For  ${}^7\text{Li}$ -projectile, the set of real parts of Woods-Saxon potentials for  $\alpha + {}^{209}\text{Bi}$  and for  $t + {}^{209}\text{Bi}$  were  $V_o = 87.93$  MeV,  $r_o = 1.361$  fm,  $a_o = 0.578$  fm and  $V_o = 130.96$  MeV,  $r_o = 1.2$  fm,  $a_o = 0.72$  fm respectively. For  ${}^6\text{Li}$ -projectile, the potentials for

TABLE 5.3: Total reaction ( $\sigma_{react.}^{total}$ ), integrated breakup ( $\sigma_{BU}^{inte.}$ ) and breakup cross sections at  $140^\circ$  ( $\sigma_{BU}^{140^\circ}$ ) from the CDCC calculation and  $\alpha$  cross sections at  $140^\circ$  ( $\sigma_\alpha^{140^\circ}$ ) from the experiment for  ${}^7\text{Li} + {}^{209}\text{Bi}$  system.

$E_{c.m.}$ (MeV)	$\sigma_{react.}^{total}$ (mb) (CDCC)	$\sigma_{BU}^{inte.}$ (mb) (CDCC)	$\sigma_{BU}^{140^\circ}$ (mb/sr) (CDCC)	$\sigma_\alpha^{140^\circ}$ (mb/sr) ( <i>Expt.</i> )
21.10	50	1	0.1	-
22.07	54	1	0.1	-
23.04	58	2	0.2	-
24.01	62	2	0.2	1±0.0
24.99	67	3	0.3	1±0.0
25.96	72	4	0.4	4±0.0
26.93	78	7	0.9	7±0.0
27.90	94	10	1.2	12±0.0
28.87	120	14	1.4	18±0.0
29.84	170	20	1.3	24±0.01
30.81	243	25	1.9	23±0.01
31.78	336	30	1.2	23±0.03
32.75	434	32	0.8	20±0.05
33.72	533	37	0.8	17±0.10
34.69	630	40	0.5	14±0.18
35.66	721	46	0.5	11±0.31
36.63	810	50	0.5	10±0.47
37.60	892	58	0.7	8±1.91

$\alpha/d + {}^{209}\text{Bi}$  were also Woods-Saxon form with  $V_o = 60.42$  MeV,  $r_o = 1.361$  fm,  $a_o = 0.578$  fm and  $V_o = 42.20$  MeV,  $r_o = 1.150$  fm,  $a_o = 0.972$  fm respectively. The imaginary parts have been taken as an internal Woods-Saxon (WS) potentials with  $W_o = 30.0$  MeV,  $r_o = 1.04$  fm and  $a_o = 0.2$  fm, to exclude the double counting of the effect of inelastic excitation on the elastic channel. The potentials for ground state of  ${}^6\text{Li}$  and bound state at  $(1/2^+, 0.478$  MeV) of  ${}^7\text{Li}$  and resonant states of  ${}^{6,7}\text{Li}$ -projectiles, have been taken from the Ref.[82]. The scattering wave functions in the solution of coupled-channels calculations were integrated up to 200 fm in steps of 0.05 fm and the relative angular momentum is taken up to  $150\hbar$ . In the present calculations, target inelastic states are not included as the effects of target inelastic states are found to be insignificant [31]. Also, the effect of transfer couplings have not been included in the present calculation as it is difficult to couple transfer channels along with the CDCC calculation because of large spin of  ${}^{209}\text{Bi}$ . In the reaction of  ${}^7\text{Li}$  with  ${}^{144}\text{Sm}$ , no effect from  $1n$ -stripping channel

was observed on the quasi-elastic scattering excitation function [41]. Tables 5.2 and 5.3 show the total reaction cross sections and BU cross sections along with the experimental  $\sigma_{\alpha}^{140^{\circ}}$ , for the  ${}^{6,7}\text{Li} + {}^{209}\text{Bi}$  systems. It can be observed from this calculation that the BU cross sections are dominant for  ${}^6\text{Li}$  as compared to that of  ${}^7\text{Li}$ . Similarly, in the Ref.[78], for the  ${}^{6,7}\text{Li} + {}^{59}\text{Co}$  systems, elastic scattering, excitation functions for sub- and near-barrier fusion cross sections, and breakup yields have been analyzed in terms of extended CDCC calculations. This also shows significant role of breakup for  ${}^6\text{Li}$  rather than  ${}^7\text{Li}$  projectile [90].

The results from the CDCC calculations are shown in the Figs. 5.5, 5.6, 5.7 and 5.8 . In these figures, the dotted line indicates the results of Coupled Channels calculations with bare potential. The continuous line shows the results of CDCC calculations for  ${}^6\text{Li}$  with elastic + direct breakup of  ${}^6\text{Li}$ . In Figs. 5.6 and 5.8 the continuous line shows the results of CDCC calculations for  ${}^7\text{Li}$  with elastic +  ${}^7\text{Li}$ -inelastic + direct breakup of  ${}^7\text{Li}$ . The fusion barrier distributions from fusion excitation functions have been shown as open circles in the Figs. 5.7 and 5.8.

These have been compared with the present quasi-elastic barrier distributions which have been obtained with the addition of BU and/or transfer to the elastic and inelastic channel. The inclusion of BU and/or transfer to the elastic and inelastic channels give a reasonable agreement with the fusion barrier distributions that have been obtained from the fusion excitation functions as shown in Figs. 5.7 and 5.8. That means in the reaction studies, involving weakly bound nuclei to extract the correct fusion barrier distribution, projectile breakup and/or transfer reaction contributions should be included in the elastic and inelastic cross sections.

### 5.4.3 Coupled Reaction Channels (CRC) Calculations

The effect from  $1n$ -stripping channel on quasi-elastic excitation function have been investigated by Coupled Reaction Channels Calculation (CRC) for  ${}^6\text{Li} + {}^{209}\text{Bi}$  reaction. Also, within this formalism a simultaneous calculation of breakup and transfer ( $1n$ -stripping) for  ${}^6\text{Li} + {}^{208}\text{Pb}$  and  ${}^{209}\text{Bi}$  systems, have been carried out

TABLE 5.4: The excitations of  ${}^{209}\text{Bi}$  included in the calculation taken from Ref.[82]

Energy (MeV)	$I^\pi$	B(E3) (W.u.)
0.0	$9/2^-$	
2.493	$3/2^+$	16.0
2.564	$9/2^+$	28.0
2.583	$7/2^+$	25.0
2.599	$11/2^+$	30.0
2.6	$13/2^+$	22.0
2.617	$5/2^+$	22.0
2.714	$15/2^+$	25.0

to understand their relative contributions as experimental results are available in the Ref.[87]. In case of weakly bound projectile, such as  ${}^6\text{Li}$  may directly breakup into two fragments ( $d + \alpha$ ) or the breakup may occur after some nucleon transfer (pickup/ stripping). Recently, in one of the experimental study involving stable weakly bound projectile ( ${}^6\text{Li}$ ) [87] the  $1n$ -stripping is found more preferable channel that leads to ( $p + \alpha$ ) and the contribution from  $1n, 1p$ -pick up is found negligible at below barrier energy in the reaction with  ${}^{207,208}\text{Pb}$  and  ${}^{209}\text{Bi}$  targets.

In the calculations for  $1n$ -stripping channel for  ${}^6\text{Li} + {}^{209}\text{Bi}$  system the energy range was from 22.0 to 39.0 MeV. Here, the  $1n$ -transfer is considered from ground state of  ${}^6\text{Li}$  to ground state of  ${}^{209}\text{Bi}$  that may lead to  ${}^5\text{Li}$  and final nucleus  ${}^{210}\text{Bi}$  in its ground state, as the Q-value for this reaction is -1.058 MeV. The effects from target ( ${}^{209}\text{Bi}$ ) excitation were also included by couplings to collective multiplet [ ${}^{208}\text{Pb}(3^-) \otimes 1h_{9/2}$ ]  $j_\pi$  as given in Table 5.4. The entrance channel potentials were of Woods-Saxon form with  $a_0=0.67$  fm and  $r_0=1.2$  fm. For the exit channel, the real part was of Akuzne-Winther type with  $a_0=0.63$  fm and  $r_0=1.167$  fm with the short range imaginary part having parameters  $W_0= 50$  MeV,  $a_0=0.4$  fm and  $r_0=1.06$  fm. The binding potentials for the valence ( $n$ ) and core ( ${}^5\text{Li}$  and  ${}^{210}\text{Bi}$ ) nuclei were of the Woods-Saxon and spin orbit form. The depths were adjusted to obtain the required binding energies. These calculations were done with spectroscopic amplitudes equal to 1.

The experimental quasi-elastic (elastic + inelastic) excitation function along with

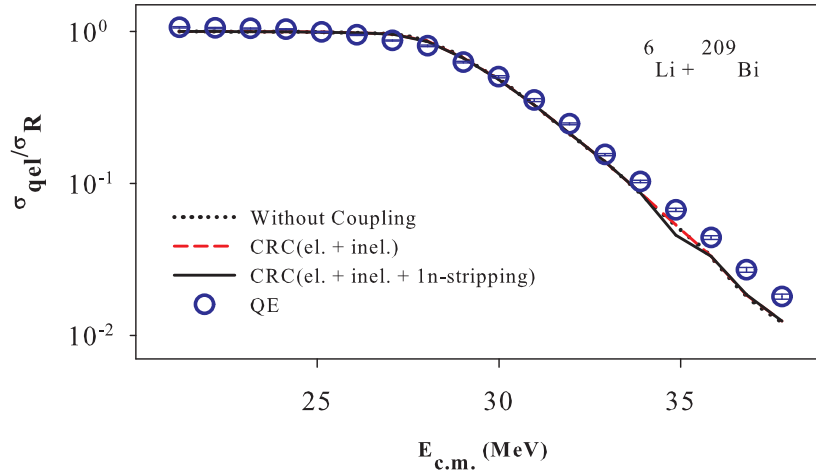


FIGURE 5.11: Quasi-elastic excitation function along with the results of 1n-stripping channel for  ${}^6\text{Li} + {}^{209}\text{Bi}$  at  $\theta_{lab} = 140^\circ$ . The dotted line indicates results obtained without any coupling. The dashed and continuous lines shows results obtained with the inclusion of target coupling and with the inclusion of target as well as 1n-stripping channel.

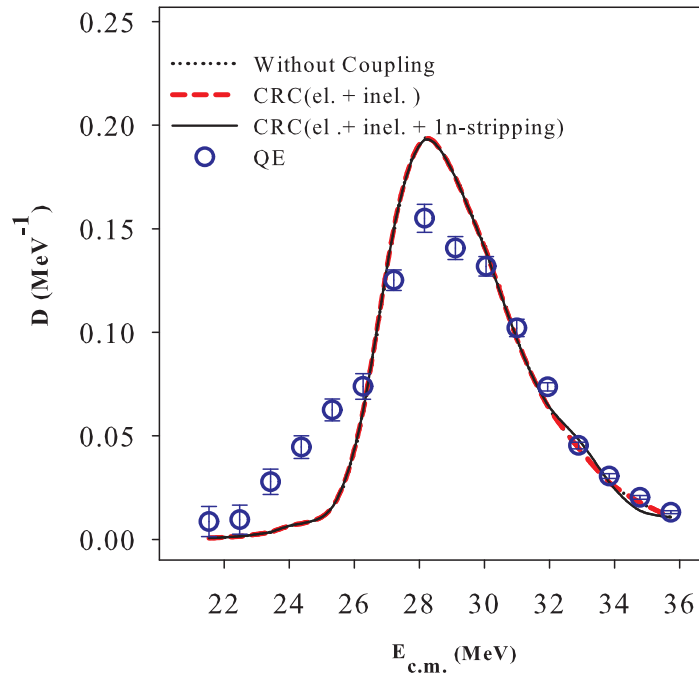


FIGURE 5.12: Corresponding barrier distribution along with the results of 1n-stripping channel for  ${}^6\text{Li} + {}^{209}\text{Bi}$  at  $\theta_{lab} = 140^\circ$ . The dotted line indicates results obtained without any coupling. The dashed and continuous lines shows results obtained with the inclusion of target coupling and with the inclusion of target as well as 1n-stripping channel.

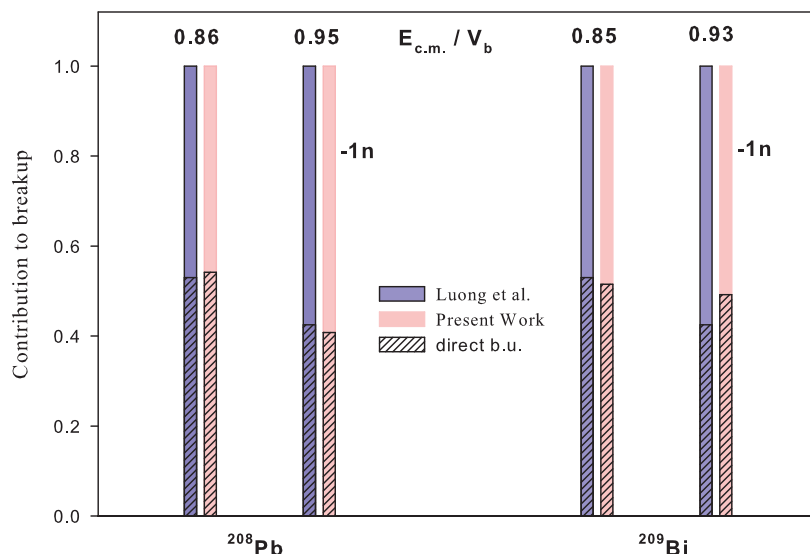


FIGURE 5.13: Relative contribution of direct breakup and  $1n$ -stripping channel in the reaction of  ${}^6\text{Li}$  with  ${}^{208}\text{Pb}$ ,  ${}^{209}\text{Bi}$

the results of coupled reaction channels calculations is shown in the Fig. 5.11. In this figure, the dotted line shows the results of CRC calculation with single channel. The dashed and continuous lines shows the excitation functions obtained with the inclusion of target inelastic and (target inelastic +  $1n$ -transfer) respectively. Fig. 5.12 shows the corresponding barrier distributions with a quite reasonable agreement between the present calculations and the experimental results.  $1n$ -transfer coupling effect on quasi-elastic excitation function is found negligible as shown in the Fig. 5.11 and similar effect can also be observed in the Fig. 5.12 with no difference in barrier distribution heights obtained with the inclusion of target inelastic and (target inelastic +  $1n$ -transfer). In a simultaneous calculations for breakup and  $1n$ -transfer in the  ${}^6\text{Li} + {}^{208}\text{Pb}$ ,  ${}^{209}\text{Bi}$  reactions, all the resonant states of  ${}^6\text{Li}$  with finer binnings and maximum excitation energy upto  $\sim 8.5$  MeV are included in the CDCC-CRC calculations. Also, the target spin is set to  $1/2^-$  to reduce the computing time. The calculations were carried out for two different laboratory energies at 26.5 and 29.0 MeV. In the present calculations, for the  $1n$ -stripping channel, coupling to ground state is considered and no target inelastic states are included as the coupling to target inelastic states give negligible cross sections. For this case, the binding energies for core and valence particles are taken

as 0.1MeV and the spectroscopic amplitudes are set at 2.0. These have been varied to obtain the neutron stripping from unbound states of  ${}^6\text{Li}$  [91].

The comparison between the results of present calculation (pink) and the experimental data as reported by Luong *et al.*, [87] are shown in the Fig. 5.13. It represents a quite reasonable agreement between the present calculations and the experimental results [92].

## 5.5 Results and Discussion

In this work, quasi-elastic scattering excitation functions have been measured at backward angles namely at  $\theta_{lab} = 140^\circ$  and  $160^\circ$  for both the  ${}^{6,7}\text{Li} + {}^{209}\text{Bi}$  systems. The fusion barrier distributions derived from experimental quasi-elastic data have been compared with the fusion barrier distributions obtained from the fusion excitation function measurements [85]. It has been observed that the final fusion barrier distributions obtained from quasi-elastic and fusion excitation function measurements are consistent only when BU and/or transfer channels are added to the quasi-elastic events. The transmission (capture probabilities) ( $T_o$ ) have also been compared with that obtained from the fusion excitation functions which indicates reasonable agreement at near barrier energies for reactions of  ${}^{6,7}\text{Li}$  with  ${}^{209}\text{Bi}$ .

From the simple Coupled Channels (CC) calculations it has been seen that the obtained barrier distributions are consistent with the experimentally measured quasi-elastic barrier distributions for both the  ${}^{6,7}\text{Li}$  with  ${}^{209}\text{Bi}$  systems but the peak positions are still lower than that obtained from the fusion excitation functions measurements. To understand these discrepancies CDCC calculations were done and breakup cross sections were added to the quasi-elastic channels. This gives better agreement with the barrier distributions from the fusion excitation functions. Further, CRC calculations are also done to understand the  $1n$ -transfer effects on fusion barrier distributions, which shows negligible effect of this channel.

Simultaneous calculation for breakup and transfer reproduces the relative contributions of breakup and  $1n$ -stripping channels reasonably well for the reaction of  ${}^6\text{Li}$  with  ${}^{208}\text{Pb}$  and  ${}^{209}\text{Bi}$ .